ADVANCING EARTH AND SPACE SCIENCES

JGR Space Physics

RESEARCH ARTICLE
10.1029/2024JA033185

Two-Spacecraft Observations of Asymmetric Martian Bow Shock: Conjunctions of Tianwen-1 and MAVEN

Long Cheng[1,2,3], Yuming Wang[1,3,4], Robert Lillis[2], Jasper Halekas[5], Benoit Langlais[6], Tielong Zhang[3,7], Jacob R. Gruesbeck[8], David L. Mitchell[2], and Shannon Curry[9]

[1]Deep Space Exploration Laboratory/School of Earth and Space Sciences, University of Science and Technology of China, Hefei, China, [2]Space Sciences Laboratory, University of California, Berkeley, Berkeley, CA, USA, [3]CAS Center for Excellence in Comparative Planetology/CAS Key Laboratory of Geospace Environment/Mengcheng National Geophysical Observatory, University of Science and Technology of China, Hefei, China, [4]Hefei National Laboratory, University of Science and Technology of China, Hefei, China, [5]Department of Physics and Astronomy, University of Iowa, Iowa City, IA, USA, [6]Nantes Université, University Angers, Le Mans Université, CNRS, Laboratoire de Planétologie et Géosciences, Nantes, France, [7]Space Research Institute, Austrian Academy of Sciences, Graz, Austria, [8]NASA Goddard Space Flight Center, Greenbelt, MD, USA, [9]Laboratory for Atmospheric and Space Physics, University of Colorado, Boulder, CO, USA

Key Points:

- We investigated the asymmetry of Martian bow shock utilizing two-spacecraft observations at distinct locations
- The dayside Martian crustal field may induce the north-south asymmetry of the bow shock
- The solar wind electric field may cause bow shock asymmetry in the Mars-Solar-Electric frame, with stronger fields increasing the effect

Correspondence to:

L. Cheng and Y. Wang,
longcheng@mail.ustc.edu.cn;
ymwang@ustc.edu.cn

Citation:

Cheng, L., Wang, Y., Lillis, R., Halekas, J., Langlais, B., Zhang, T., et al. (2024). Two-spacecraft observations of asymmetric Martian bow shock: Conjunctions of Tianwen-1 and MAVEN. *Journal of Geophysical Research: Space Physics*, *129*, e2024JA033185. https://doi.org/10.1029/2024JA033185

Received 15 AUG 2024
Accepted 10 SEP 2024

Abstract

The Martian bow shock has been extensively studied through magnetic field and plasma instrument observations from various Mars space missions. However, prior investigations primarily involve statistical analyses based on single spacecraft crossings, leaving the asymmetry of the Martian bow shock unstudied through simultaneous two-spacecraft observations. In this study, utilizing simultaneous observations from Tianwen-1 and MAVEN, we examine the instantaneous asymmetry of the Martian bow shock. We present the asymmetry of the Martian bow shock in the Mars-Solar-Electric and Mars-Solar-Orbital reference frames, possibly influenced by the solar wind motional electric field and Martian crustal magnetic field, respectively. Moreover, we suggest that the bow shock exhibits increased asymmetry under stronger solar wind motional electric field conditions. This study highlights how a two-point observation approach offers valuable insights into the dynamic behavior of the Martian induced magnetosphere.

Plain Language Summary

Scientists have been studying the Martian bow shock, which slows down the solar wind from supersonic to subsonic, using instruments on different Mars missions. But most studies only use data from one spacecraft, so we don't know much about how the bow shock varies in different places at the same time. In this study, we looked at data from two spacecraft, Tianwen-1 and MAVEN, at the same time to see if we could find any differences. We found that the bow shock is different in the northern and southern parts of Mars in different reference frames, and this might be because of the solar wind electric field and the Martian crustal field. We also noticed that the bow shock is more different when the solar wind electric field is stronger. Such two-spacecraft observations helps us understand more about how the magnetic environment around Mars works.

1. Introduction

The Martian bow shock (BS) is where the supermagnetosonic solar wind drops to submagnetosonic and deflects around the planetary obstacle (for instance, (Mazelle et al., 2004)). The Martian BS serves as the first interface between the solar wind and the Martian magnetosphere. Variations of the location and geometry of the Martian BS reflect the dynamic interaction between the solar wind and Mars. The location of the Martian BS has been widely investigated through observations of Mariner 4, Mars 2, 3, 5, Phobos 2, Mars Global Surveyor (MGS), Mars Express (MEX) and Mars Atmosphere Volatile EvolutioN (MAVEN) missions, and numerous models of the BS location have been proposed (e.g., (Edberg et al., 2008; Gruesbeck et al., 2018; Trotignon et al., 2006; Vignes et al., 2000)). The global position and shape of the Martian BS varies with the solar cycle (Hall et al., 2016, 2019), and is mainly affected by the solar extreme ultraviolet flux, solar wind Mach number, dynamic pressure and the Martian crustal fields (Garnier, Jacquey, Gendre, Genot, et al., 2022). Though most models of the Martian BS location simplify the BS surface as a symmetric conic surface, the asymmetry of the Martian BS and its drivers has also been investigated.

The BS asymmetry caused by the crustal magnetic fields was first revealed by MGS observations (Mazelle et al., 2004). The strongest magnetized crustal region located in the southern hemisphere, which is centered on about −45° latitude and 180° longitude in the IAU Mars reference frame, may induce differences between BS locations between the northern and southern hemispheres. Edberg et al. (2008) observed that, on a global scale, the BS crossings observed in the southern hemisphere are located further from the planet than the northern hemisphere crossings; however, no clear distinction was found between weak and strong crustal field regions. Halekas et al. (2017) also suggested a weak dependence on subsolar longitude due to the crustal fields. The magnetohydrodynamic (MHD) simulation performed by Fang et al. (2017) suggested that the crustal field effects cannot be simply parameterized by the subsolar longitude and BS locations are collectively affected by the global crustal field distribution. Gruesbeck et al. (2018) showed that the dayside location of the strong magnetized crustal region in the southern hemisphere may cause the north-south asymmetry. Considering various conclusions on the influence of crustal magnetic fields on the Martian BS location from previous studies, Garnier, Jacquey, Gendre, Génot, et al. (2022) conducted an analysis in detail, combining MAVEN and MEX observations. They found that the influence decreases with angular distance to the strongest crustal field region in the southern hemisphere. The influence is modulated by the local time of the strongest source region, with no influence past the terminator. The influence is also affected by the interplanetary magnetic field (IMF), which is maximized when the IMF is stable.

The influence of the IMF orientation on the BS asymmetry has been discussed at Venus, Earth and also Mars (Garnier, Jacquey, Gendre, Genot, et al., 2022). Vignes et al. (2002) suggested that the BS is farther from Mars in the hemisphere where the solar wind motional electric field is locally upward, which may be related to mass loading of picked-up oxygen ions in that hemisphere (Dong et al., 2015; Fang et al., 2008). Edberg, Brain, et al. (2009) also suggested that the BS in the hemisphere of locally upward convective electric field is statistically higher than that in the hemisphere of locally downward convective electric field. The MHD simulation performed by Wang et al. (2020) also investigated the effects of IMF on BS location, finding that the cross section of BS is elongated in the direction perpendicular to the IMF on the Y–Z plane. Sui et al. (2023) found that the terminator section of the BS is elongated in the pole directions under the B_y condition. Garnier, Jacquey, Gendre, Genot, et al. (2022) demonstrated a small shock asymmetry in the Mars Sun Electric (MSE) reference frame. They also suggested that the asymmetry is stronger at larger cone angles, as the solar wind motional electric field $-\boldsymbol{V} \times \boldsymbol{B}$ is increased and may accelerate pickup ions and increase the mass loading and thus the size of the obstacle to the solar wind. Unpaired Student's *t*-tests were performed to infirm the presence of a north versus south asymmetry.

Up to now, the asymmetry of the Martian BS has mostly been investigated using data sets of BS crossings at different times by single spacecraft. However, single-spacecraft observations limit the direct evidence of an instantaneously asymmetric Martian BS, which is only available via two-point observations where two spacecraft cross the BS at different locations. Edberg, Eriksson, et al. (2009) presented the first two-spacecraft near-simultaneous observations of the Martian BS by Rosetta and Mars Express. The time difference of BS crossings were at scale of hours and there was no obvious BS asymmetry in the case. In addition, two-spacecraft observations enable quantitative studies of the BS asymmetry, as the asymmetry level and corresponding driver (e.g., the solar wind motional electric field) can be estimated and correlated. In this study, we gain new insights into the asymmetry of the Martian BS, utilizing simultaneous observations of Tianwen-1 and MAVEN, which is a powerful tool for studies of the Martian space environment (Cheng et al., 2023).

2. Observations

During the initial two month of Tianwen-1 scientific observations, spanning from Mid-November of 2021 to Mid-January of 2022, both Tianwen-1 and MAVEN transited between the solar wind and the magnetosheath, resulting in frequent crossings of the Martian BS (see Figure 1 in Cheng et al. (2023)). We manually identified the shock crossings of Tianwen-1 and MAVEN, utilizing magnetic field measurements from Tianwen-1/MOMAG (Liu et al., 2020; Wang et al., 2023, 2024; Zou et al., 2023) and magnetic field, ion and electron measurements from MAVEN/MAG (Connerney et al., 2015), SWIA (Halekas et al., 2015) and SWEA (Mitchell et al., 2016), respectively (see Section 3 for details). By analyzing two crossings occurring in close temporal proximity but at different hemispheres/locations, we intend to investigate the instantaneous asymmetry of the BS. To mitigate the impact of shock motion during the time delay between the two spacecraft's crossings, we specifically selected 11 events where Tianwen-1 and MAVEN crossed the shock within a three-minute timeframe. Then we further select the events that indicate asymmetric shock, based on the method described below.

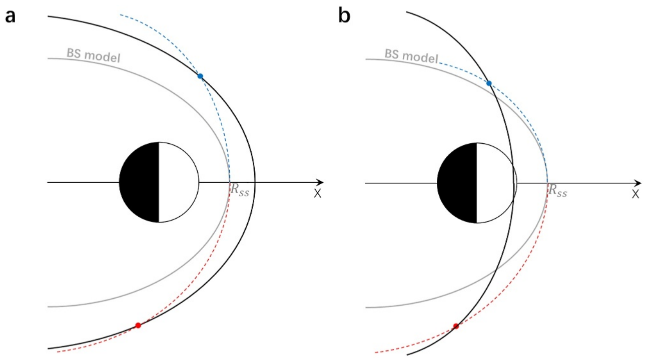

Figure 1. Schematic illustrations of the bow shock event that (a) can be explained by both asymmetric bow shock geometry and scaled bow shock geometry, and (b) can only be explained by asymmetric bow shock geometry. The MSO X axis points from Mars' center to the Sun. The gray line represents the location of certain bow shock model, where R_{ss} indicates the location of the subsolar point. The dashed lines in different hemispheres represent the conic line crossing R_{ss} and the location of the shock crossing in the hemisphere. The black conic line crosses the locations of the shock crossing at different hemispheres.

3. Selection of Asymmetric Bow Shock Events

Usually, modeling of the Martian bow shock assumes a symmetric shock surface around the main axis, X', which is the 4°-aberrated X axis of the Mars-Solar-Orbital (MSO) frame. Statistical analyses involve fitting locations of shock crossings by a spacecraft with a conic line in MSO cylindrical coordinates. The shock asymmetry can also be investigated by statistical studies. Previous research, for instance, separately fit shock locations recorded by the spacecraft in the MSO northern and southern hemispheres. These studies found that the average shock locations differed between hemispheres, indicating a north-south asymmetry in MSO frame.

Typically, the 2D conic function for the bow shock is with three parameters, the eccentricity ϵ, the semilatus rectum L and the focus point x_F. As described in Section 2.2.1 in Simon Wedlund et al. (2022), such a 2D conic takes the form:

$$r = \frac{L}{1 + \epsilon \cos \theta}, \tag{1}$$

where r is the distance to the shock surface from the focus point and θ is the angle measured from the focus point:

$$r = \sqrt{(X' - x_F)^2 + Y'^2 + Z^2}, \tag{2}$$

$$\cos \theta = \frac{X' - x_F}{r}. \tag{3}$$

The equivalent rectangular form is:

$$R = \sqrt{(\epsilon^2 - 1)(X' - x_F)^2 + 2\epsilon L\left(X' - x_F\right) - L^2}, \tag{4}$$

where $R = \sqrt{Y'^2 + Z'^2}$ is the distance from the shock surface to the main axis.

Ramstad et al. (2017) rewrote this conic function as a function with parameters of the eccentricity, the subsolar point R_{ss} and a scale length α that is kept constant using the value $\alpha = 33.5\ R_M$ found by Vignes et al. (2000), which results in two free parameters.

$$R = \alpha\sqrt{\epsilon^2 - 1}\sqrt{\frac{(X' - R_{ss} - \alpha)^2}{\alpha^2} - 1}. \tag{5}$$

Based on the coordinates of shock crossings, $\left(X_i', Y_i', Z_i'\right)$, we can fit the optimum conic parameters through minimizing the χ-squared value:

$$\min \sum \left(\sqrt{Y'^2_i + Z'^2_i} - R\right)^2. \tag{6}$$

Utilizing shock locations of Tianwen-1 and MAVEN crossings, we can fit the two parameters in Equation 5.

Similar to the definition of the clock angle of the magnetic field vector in MSO, which is calculated by $\tan^{-1}(B_y/B_z)$ and means the angle from $+Z$ to $+Y$ axis, we could define $\tan^{-1}(P_y/P_z)$ as the "clock angle" of the location of the spacecraft, where P_y and P_z are the spacecraft coordinates in MSO Y and Z axis respectively. Under the assumption of symmetric bow shock, the conic parameters are invariant at locations with different "clock angles". For a description of the asymmetric bow shock, the conic parameters are functions of the "clock angle".

Table 1
Parameters of the Spacecraft and the Upstream Solar Wind for the Events

No.	S/C	UTC	S/C MSO Lat (°)	S/C MSE clock (°)	Anomaly MSO Lon (°)	IMF strength (nT)	IMF cone (°)	SW speed (km/s)	SW density (cm^{-3})	SW P_{dyn} (nPa)	SW M_{ms}	SW $\lvert E \rvert$ (mV/m)	BS θ_{Bn}(°)	BS ΔR_{ss} (R_M)
1	TW1	2021-12-11/ 13:18:31	−57.5	−17.5	101.8	7.3	103.5	410.7	3.4	0.97	3.42	2.95	63.3	0.39
	MVN	2021-12-11/ 13:19:38	51.3	95.2									80.6	
2	TW1	2021-12-16/ 19:43:20	−19.9	−114.4	135.7	6.4	120.2	502.7	5.3	2.23	4.45	2.29	27.6	0.19
	MVN	2021-12-16/ 19:41:50	51.3	−39.9									20.8	
3	TW1	2021-12-17/ 02:44:42	−16.6	−89.1	−145.3	3.3	114.7	498.7	2.3	0.94	5.64	1.29	21.4	0.03
	MVN	2021-12-17/ 02:44:50	55.5	−16.1									42.4	
	MVN	2021-12-29/ 15:42:00	−5.0	50.7									38.1	
4	TW1	2022-01-01/ 18:08:19	−100.3	113.8	−25.2	2.3	65.3	455.2	2.4	0.82	5.94	0.75	10.4	0.12
	MVN	2022-01-01/ 18:10:35	−98.8	−166.5									66.1	
5	TW1	2021-12-29/ 15:40:02	−79.2	−32.9	−39.3	6.3	48.8	275.1	5.4	0.68	1.67	1.08	84.4	0.41
	MVN	2021-12-29/ 15:42:00	−5.0	50.7									38.1	

Note. The columns show the indices of the cases, the spacecraft (Tianwen-1 or MAVEN), time of the bow shock crossing, latitude of the spacecraft in MSO, "clock angle" of the spacecraft in MSE, longitude of the strongest region of the Martian crustal field (45°S, 180°E in the geographical coordinate system), strength and cone angle (in MSO) of the IMF, solar wind speed, density, dynamic pressure, fast magnetosonic Mach number, strength of the solar wind motional electric field, θ_{Bn} and ΔR_{ss} of the bow shock.

For shock crossings of Tianwen-1 and MAVEN at different "clock angles", it is hard to estimate the conic parameters at each "clock angle" from only corresponding location. Despite potential differences in the conic parameters for the bow shocks at Tianwen-1 and MAVEN, it's crucial to note that at any given moment, the bow shock has only one subsolar point. Based on the two-parameter conic function mentioned above, we can estimate the shock geometry by the location of spacecraft's crossing and the assumed subsolar point.

The difference of the derived shock geometries at locations of Tianwen-1 and MAVEN crossings may reveal the shock asymmetry. However, we found that the unsure subsolar location may affect the result. For example, for the event illustrated by Figure 1a, where the red and blue points show the two locations of the shock crossings of two spacecraft, if we assume subsolar point of the shock model as the actual subsolar point, we have two different derived shock geometry at each location (see the red and line dashed lines), which are asymmetric around the main axis of the bow shock. However, we can find a subsolar point that makes the derived shock geometry being symmetric around the main axis (see the black solid line). Actually, such point is just the subsolar point of the conic line that fits the two locations of spacecraft crossings, where the bow shock geometry is scaled. Hence, the shock locations in Figure 1a can be explained by both the asymmetric shock and the scaled shock.

The situation in Figure 1b is different from Figure 1a. Here, if we assumed the subsolar of the shock model as the one at the moment of spacecraft crossings, the shock geometry at the two individual locations are asymmetric (see the red and line dashed lines). We can also derive the scaled bow shock that crosses the spacecraft locations (see the black solid line). However, in this case, the scaled bow shock is unrealistic, as its subsolar location is even less than 1 R_M. Hence, the distinct shock locations in this case can only be explained by the shock asymmetry. We only choose similar events for studies on the shock asymmetry. Table 1 lists the information of the five events we found, which will be further analyzed in the next section.

4. Analysis

Here we look at the five case studies, where the first three (Events 1–3) implies a solar wind electric field effect and the last two (Events 4 and 5) a Martian crustal field effect.

4.1. Asymmetry Explained by the Solar Wind Motional Electric Field

Figure 2 shows an event (Event 1) during which Tianwen-1 and MAVEN crossed the BS at nearly the same time, ∼13:20UT on 2021 December 11. As shown in Figure 2c, during the period of this event, Tianwen-1 entered the solar wind at 13:18:17UT, crossing the BS from the magnetosheath side. The magnetic field strength, $|B|$, abruptly decreased from ∼16 to ∼9 nT. The spectrum of the magnetic field shows expected differences across the BS, that is, from the turbulent magnetosheath to the steadier solar wind. As shown in Figure 2d, during the period of this event, MAVEN also moved from the magnetosheath to the solar wind. MAVEN entered the solar wind at 13:19:38UT, with $|B|$ changing from 15 to 7 nT. The magnetic field spectrum also shows expected sheath turbulence, while foreshock disturbances are observed in the spectrum between 13:20UT and 13:25UT. MAVEN crossings of the BS can also be identified from the discontinuities in the solar wind proton energy spectrum, the derived solar wind density and velocity (Figure 2d, panels 4–6), and the solar wind electron energy spectrum (panel 7).

Tianwen-1 and MAVEN crossed the BS in the southern and northern hemispheres respectively, with latitudes in the MSO frame of −57° and 51° (listed in Table 1). Both Tianwen-1 and MAVEN crossed the BS near the terminator (see Figure 2a). Locations of the BS and magnetic pileup boundary from the model of Edberg et al. (2008) are shown in Figure 2a for reference. As expected, locations of BS crossings of Tianwen-1 and MAVEN both deviated from the BS model. While the location of MAVEN's crossing was close to the BS model, Tianwen-1's was farther from Mars. As illustrated by Figure 1, we fitted the locations of Tianwen-1 and MAVEN crossings with a conic section, while the resulting combined BS shape is shown by the magenta line in Figure 2a. The implied subsolar location of the fitted BS is much closer to Mars than is physically reasonable, with X position of about 1.1 R_M, which is even smaller than the modeled location of the magnetic pileup boundary. This unreasonable fitted BS location indicates the asymmetry of the BS at locations of Tianwen-1 and MAVEN crossings, where the BS at Tianwen-1 crossing is farther from Mars. It is noteworthy that both Tianwen-1 and MAVEN crossed the BS multiple times during the period of event. Locations of each crossing are shown in Figure 2a. The small difference between the multiple crossings would not affect the explanation of asymmetric BS.

Figure 2b shows locations of Tianwen-1 and MAVEN crossings in the MSE Y-Z plane. MAVEN crossings were located near the equator (X-Y plane), while Tianwen-1 crossings were located in the northern hemisphere and near the $+Z$ direction (i.e., the direction of the solar wind motional electric field). The radial component of the crustal magnetic field at 400 km altitude predicted by the Martian crustal field model of Langlais et al. (2019) is also overlaid in the figure. During the period of interest, the strongest magnetized crustal region was in the nightside. The farther-out location of Tianwen-1 crossings can be explained by the solar wind motional electric field. Dong et al. (2015) presented the ion plume organized by the upstream solar wind motional electric field. The ion plume is along the upstream electric field over the north-pole region of the MSE reference frame. The ion plume may push the BS at the MSE northern hemisphere farther from Mars, which results in a north-south asymmetry in the MSE reference frame.

Figures 3 and 4 show two other events (Events 2 and 3) that may be explained by the north-south asymmetry in the MSE reference frame, which further suggest the effect of the ion plume on the BS shape. For Event 2 shown in Figure 3, MAVEN crossed near the equator while Tianwen-1 crossed in the northern hemisphere (see Figure 3b). The location of Tianwen-1's crossing was inside the BS model and that of MAVEN was outside the model (see Figure 3a). Here we did not show the fitted BS shape as it would be completely unphysical, with the subsolar point being infinitely far from Mars. It is therefore clear that the BS at the location of MAVEN is more inflated than that of Tianwen-1. Event 3, shown in Figure 4, is similar to Event 2. The location of MAVEN's crossing was near the MSE $+ Z$ direction and was farther from Mars, which can also be explained by the ion plume.

4.2. Asymmetry Explained by Mars' Crustal Magnetic Field

Figure 5 shows an event (Event 4) that may exhibit the north-south asymmetry of the BS in the Mars Solar Orbital (MSO) reference frame. During the period of interest, Tianwen-1 moved from the magnetosheath to the solar wind, with the magnetic field being steadier. Tianwen-1 first crossed the BS at 18:08:05UT, characterized by

10.1029/2024JA033185

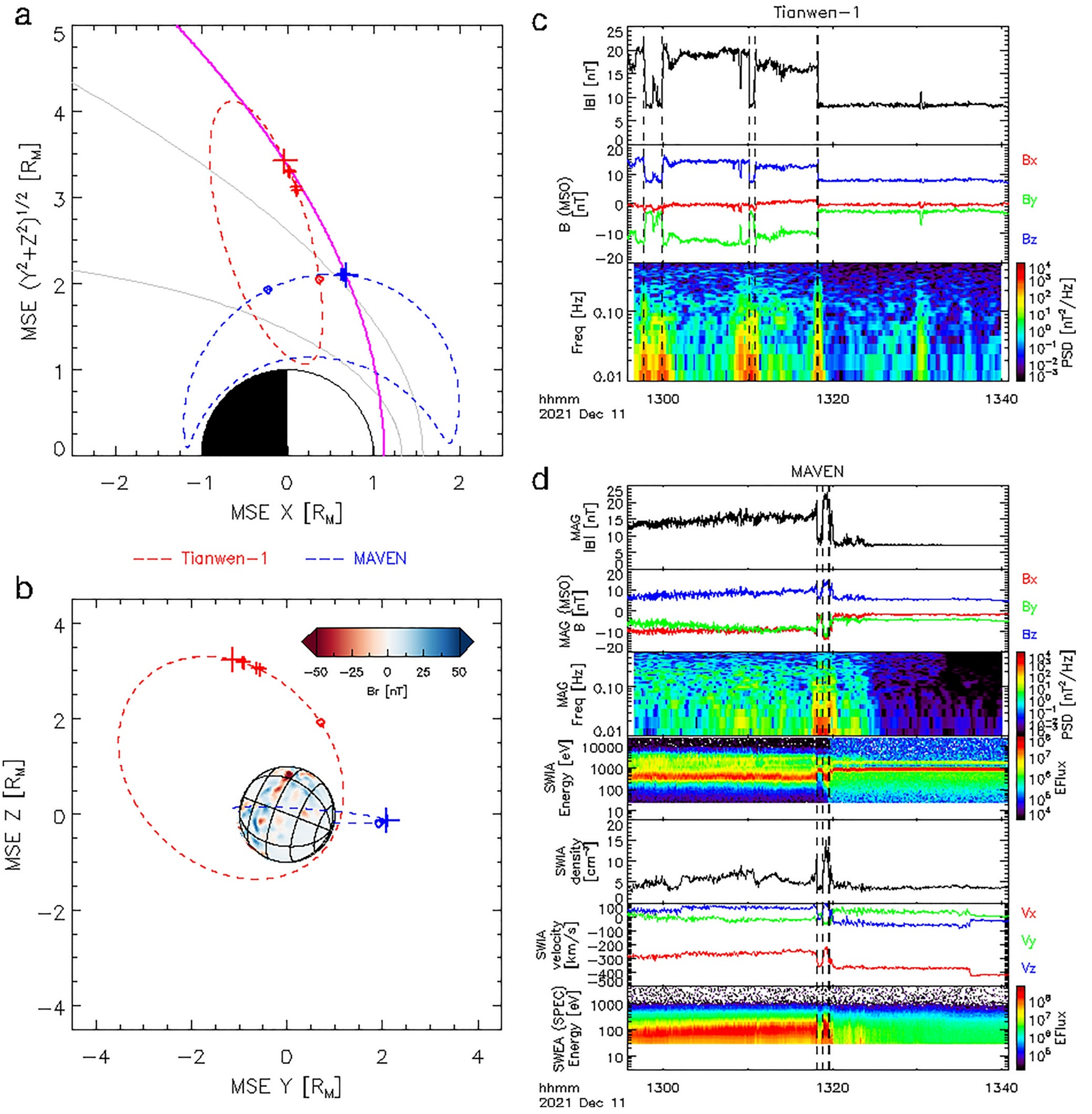

Figure 2. Tianwen-1 and MAVEN observations of the asymmetric BS event on 2021 December 11. (a) Trajectories of the orbiters (dashed lines), locations of the BS crossings (cross symbols) and magnetic pileup boundaries (diamond symbols) in MSE cylindrical coordinates, with red and blue for Tianwen-1 and MAVEN respectively. Locations of the BS and magnetic pileup boundary from Edberg et al. (2008) are shown by the gray lines for reference. The magenta line represents the conic line fitted by the BS crossings. (b) Trajectories of the orbiters (dashed lines), locations of the BS crossings (cross symbols) and magnetic pileup boundaries (diamond symbols) in the MSE *Y-Z* plane. Map of the radial component of the Martian crustal field (Langlais et al., 2019) at 400 km altitude is overlaid. (c) Tianwen-1 observations during the event, where subpanels from top to bottom show the magnetic field strength, three components of the magnetic field in MSO coordinates, and the power spectral density (PSD) of the magnetic field strength. (d) MAVEN observations, where the top subpanels are similar to those in panel (c) and the rest show the proton energy spectra with unit in the energy flux, eV/(eV·cm^2·s·sr), the onboard derived solar wind density, velocity in MSO coordinates, and the electron energy spectra. The vertical dashed lines show the time of the BS crossings.

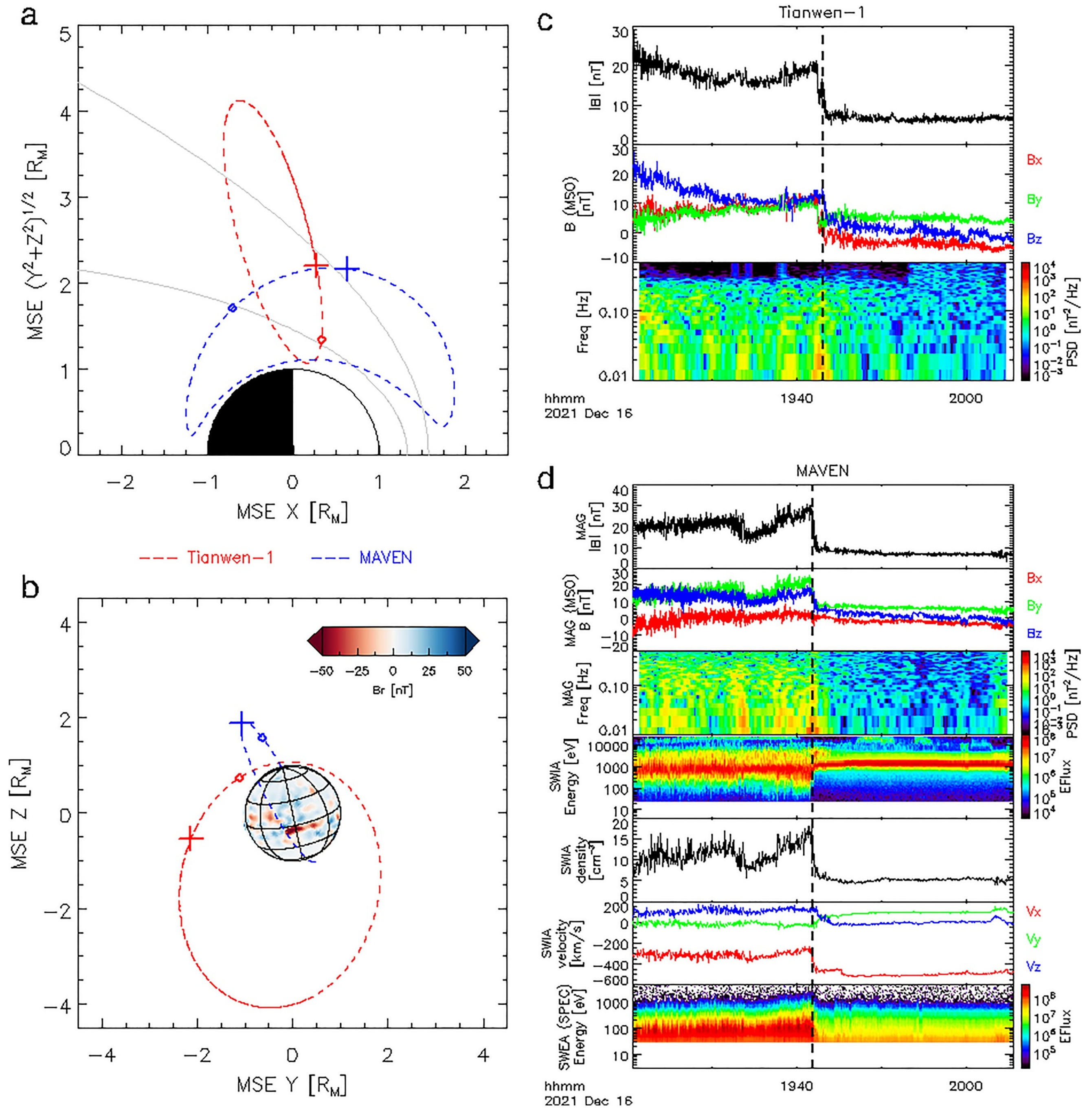

Figure 3. Similar to Figure 2 but for the event on 2021 December 16.

discontinuities in the strength, components and spectrum of the magnetic field (see Figure 5c). MAVEN crossed the BS from the solar wind to the magnetosheath at 18:10:35UT, where $|B|$ decreased from ∼10 to ∼3 nT, with corresponding changes in the three components. Discontinuities at the BS are also obvious in the energy spectrum of the solar wind proton and electron (see Figure 5d). The increased density and decreased speed indicate the compression and deflection of the solar wind beams. Tianwen-1 crossed the BS in the southern hemisphere but near the equator in the MSO reference frame, while MAVEN crossed the BS in the northern hemisphere (see Figure 5b). The location of Tianwen-1 crossing was closer to the Edberg's BS model and that of MAVEN deviated from the BS model more (see Figure 5a). It can be inferred that the BS at Tianwen-1 crossing was more inflated than that at MAVEN crossing.

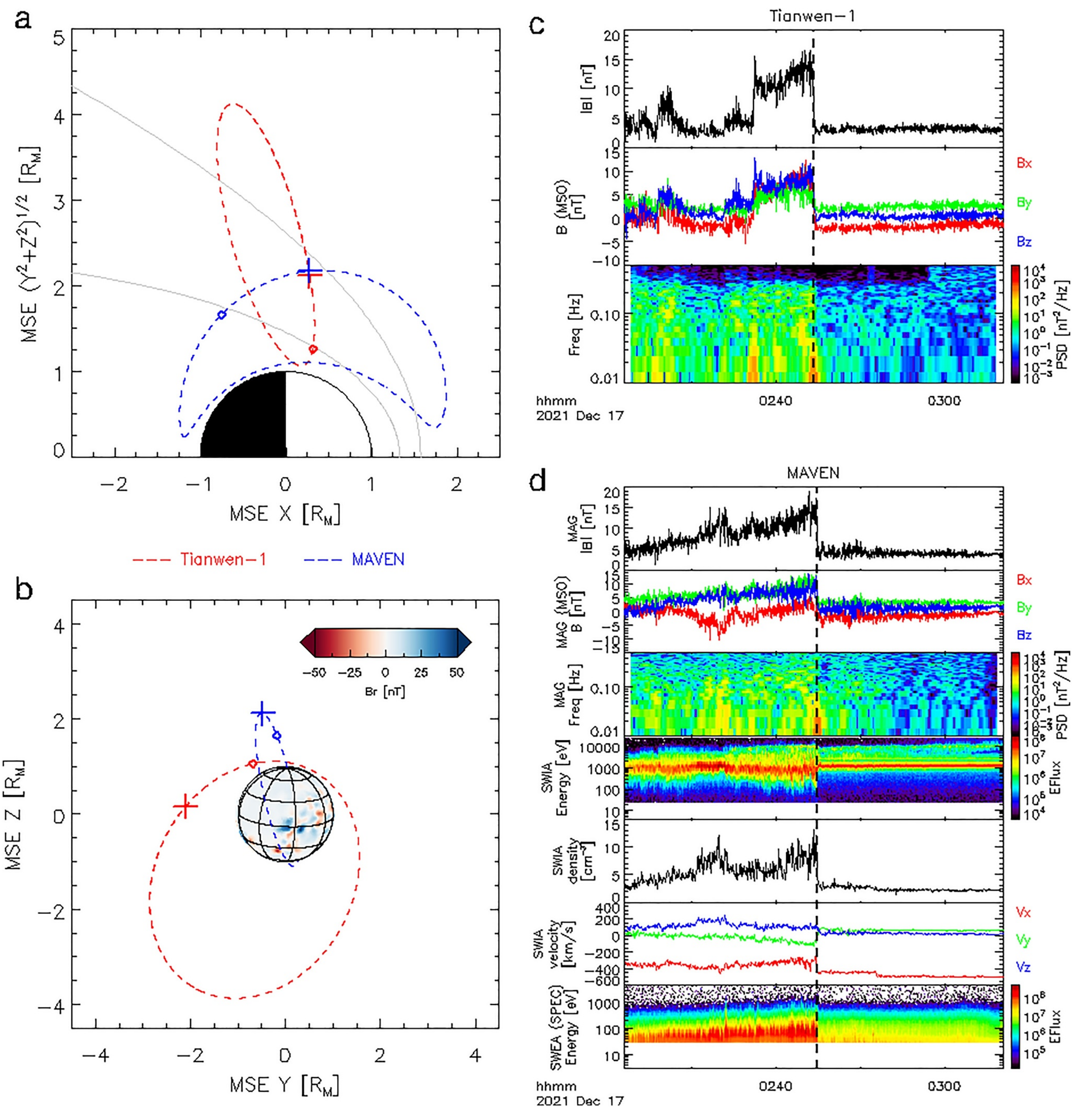

Figure 4. Similar to Figure 1 but for the event on 2021 December 17.

For this case, both Tianwen-1 and MAVEN crossings are located in the MSE southern hemisphere (see Figures 5b and 5Table 1). Hence, the ion plume may not explain the asymmetry in this case. The map of the Martian crustal magnetic field, which rotates with Mars, at the moment of BS crossings, is also shown in Figure 5b. During the period of interest, the longitude of the strongest magnetized crustal region (centered on about 45°S and 180°E in the geographic coordinates) in MSO frame was about −25°. In the MSO *Y-Z* plane viewed from the Sun, the strong crustal field region was on the dayside (see Figure 5b). At the moment of BS crossings, the crustal field in the dayside showed notable north-south differences. The dayside strong crustal field at the southern hemisphere may push the BS farther from Mars, hence the BS at the northern hemisphere is relatively closer to Mars, which could explain the BS asymmetry in this case.

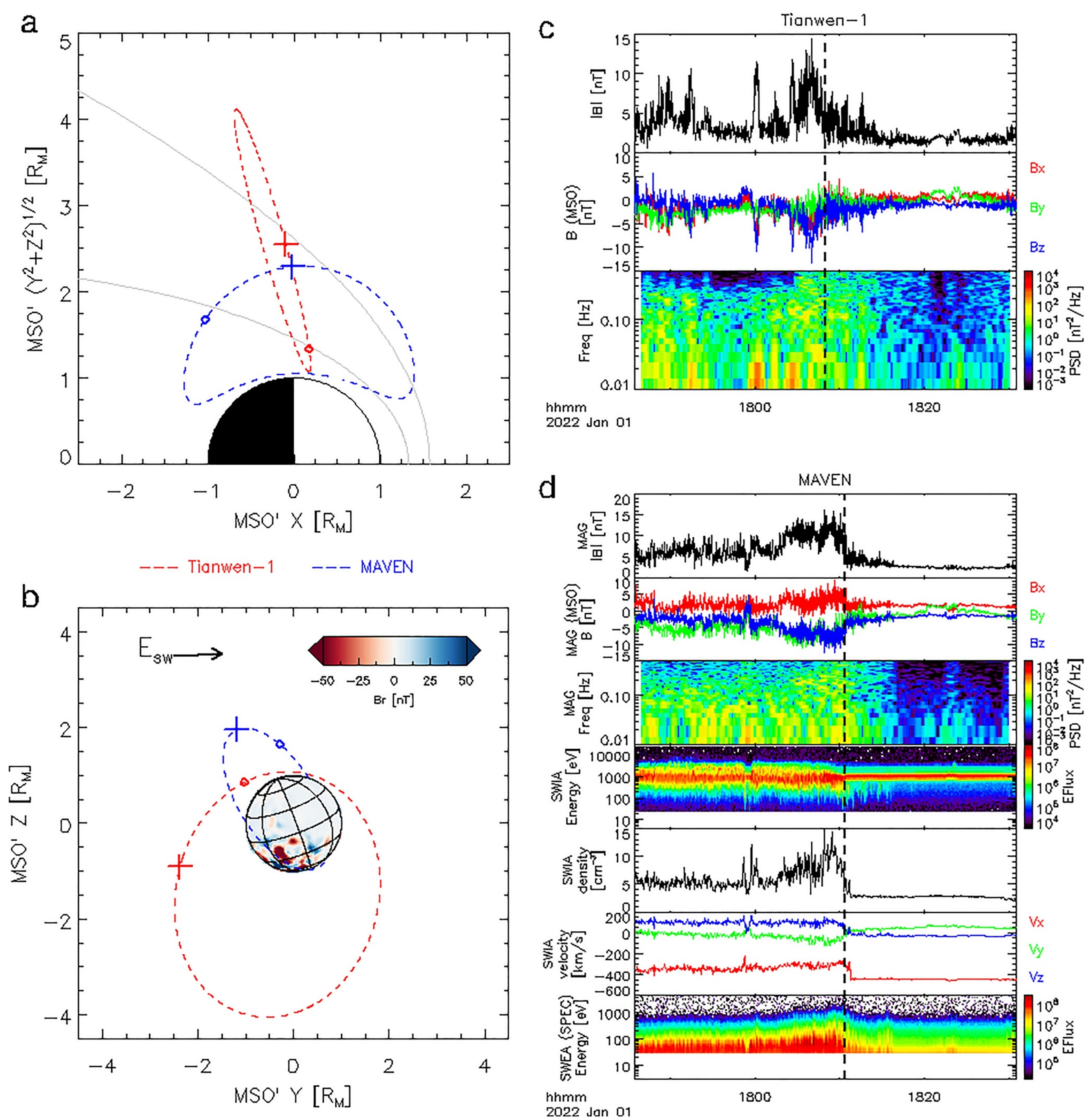

Figure 5. The asymmetric BS event on 2022 January 1. The panels are similar to those in Figure 2, where the reference frame for panels (a) and (b) is the MSO reference frame. Map of the radial component of the Martian crustal field (Langlais et al., 2019) at 400 km altitude is overlaid on the Mars in panel (b). The arrow in panel (b) shows the direction of the solar wind motional electric field.

Figure 6 shows another event (Event 5) that may indicate the BS asymmetry caused by the Martian crustal field. For this case, the BS at Tianwen-1 crossing in the southern hemisphere seems more inflated than that of MAVEN near the equator, as the fitting-resulted BS subsolar point is close to that of the BS model, but the eccentricity quite differs from the model (see the magenta line in Figure 6b). Typically, for an inflated BS, both the subsolar point and the eccentricity increase, while for a shrunk BS, both the subsolar point and the eccentricity decrease (Ramstad et al., 2017). Hence, we infer that the BS crossed by Tianwen-1 and MAVEN may also be asymmetric in this case and may be caused by the dayside Martian strong crustal field.

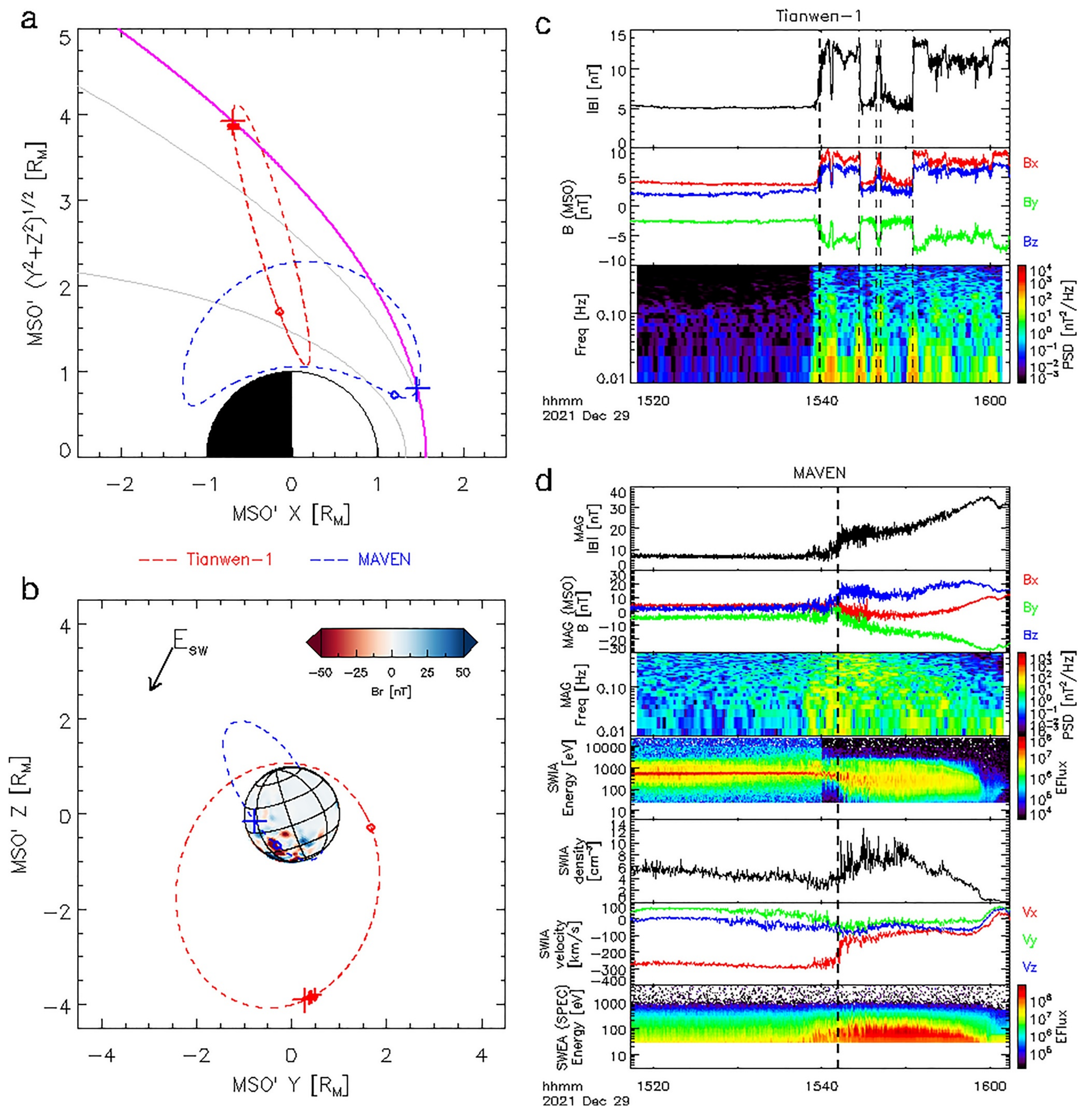

Figure 6. Similar to Figure 1 but for the event on 2021 December 29.

5. Discussion

Figure 7 schematically illustrates effects of the Martian ion plume and crustal field on the BS. As shown in Figure 7a, in the MSE reference frame, the ion plume points the $+Z$ direction, due to the solar wind motional electric field. The ion plume may push the BS in the $+Z$ direction to a location farther from Mars (the red line), which results in the north-south asymmetry in the MSE reference frame. For Events 1–3 observed by Tianwen-1 and MAVEN, a plausible explanation is that the BS detected by one spacecraft in the northern hemisphere is more inflated than the BS detected by the other spacecraft near the equator.

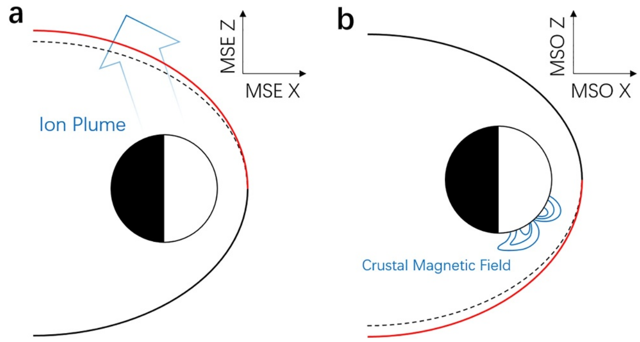

Figure 7. Schematic illustrations of the BS asymmetry caused by (a) the ion plume and (b) the Martian crustal field. The reference frame for panels (a) and (b) are the MSO and MSE reference frame respectively. The dashed conic line and the solid black one are symmetric about the *X* axis. The red line indicates the BS at higher altitudes.

The irregular Martian crustal field may also result in the asymmetry of the BS. As shown in Figure 7b, in the MSO reference frame, when the crustal field rotates to the dayside, the strong crustal field region in the southern hemisphere may push the BS in the southern hemisphere farther from Mars (the red line), which may induce the north-south asymmetry in the MSO reference frame. For Events 4 and five observed by Tianwen-1 and MAVEN, the BS detected by one spacecraft in the southern hemisphere would be more inflated than the BS detected by the other spacecraft in the northern hemisphere or near the equator.

It is noteworthy that, for Events 1–3, during the period of each event, the strong crustal field region of Mars was on the nightside, that is, the MSO longitudes of the strong crustal fields were larger than 90° or less than −90° (see Table 1). The dayside crustal magnetic field was weak, as shown in Figures 2b, 3b and 4b. Hence, it is reasonable to exclude the crustal field as a primary cause of the BS asymmetry and instead attribute the asymmetry in Events 1–3 to the solar wind motional electric field. For Events 4 and 5, we propose that the BS asymmetry is explained by the crustal field, as the strong crustal field region was at the dayside. We discount the effect of the solar wind motional electric field on the asymmetry observed in these two events because (a) the locations of both Tianwen-1 and MAVEN crossings of the BS were in the same hemisphere in MSE and nearly asymmetric around the solar wind motional electric field direction and (b) the strength of the solar wind motional electric field was relatively weak, which may have little effect on the BS asymmetry, according to the analysis in the next paragraph.

Compared to statistical studies on the BS asymmetry from single spacecraft observations, two-spacecraft observations enable quantitative analysis of the BS asymmetry. We first define a factor for estimating the BS asymmetry level at two locations (blue and red points in Figure 8a). For each location, we scaled the modeled BS curve to a curve that crosses the actual BS crossing. The scaled conic line has the same eccentricity as the model one, while the semilatus rectum and the focus point are scaled by the factor σ. The scaled lines for the two actual locations are with different scaled factors, σ_1 and σ_2. The locations of the resulting subsolar point are $\sigma_1 R_{ss}$ and $\sigma_2 R_{ss}$ respectively, where R_{ss} is the location of the subsolar point of the BS model. We define the difference between the two subsolar points, ΔR_{ss}, as the factor for the BS asymmetry level. Larger ΔR_{ss} indicates that the BS is more asymmetric. The results for each event are shown in Table 1. For Events 1–3 that possibly reflect the BS asymmetry caused by the solar wind motional electric field, we can quantitatively investigate the relation between the BS asymmetry and the strength of the solar wind motional electric field, E_{mot}. The result is shown in Figure 8b. Interestingly, the BS is more asymmetric under stronger solar wind motional electric field. While E_{mot} increases from ∼1.3 to ∼3 mV/m, ΔR_{ss} increases from ∼0.03 to ∼0.4 R_{M}.

Nevertheless, similar to the location of the BS, the asymmetry of the BS observed by two spacecraft may be a function of other variables, including solar wind parameters, locations of the Martian crustal field and locations

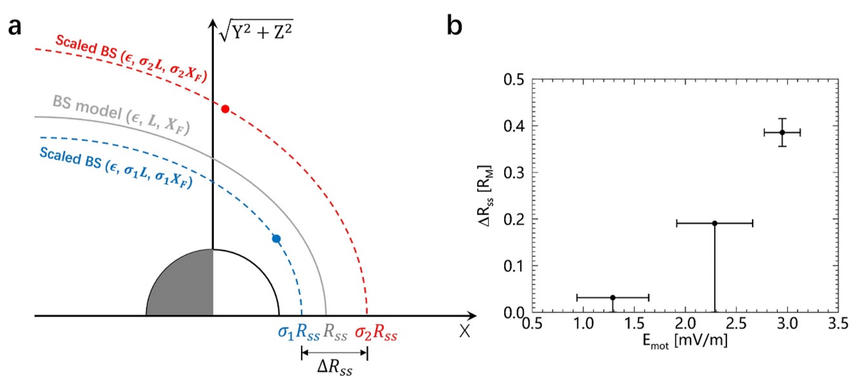

Figure 8. (a) Schematic illustration of the factor for the BS asymmetry level, ΔR_{ss}. (b) Relation between ΔR_{ss} and the strength of the solar wind motional electric field, E_{mot}, resulted from Events 1–3.

the BS crossed by the individual spacecraft. We speculate that the Martian crustal field and the solar wind motional electric field are the two primary drivers for the BS asymmetry. However, for the same condition of these two drivers, the asymmetry of the BS may be different under different other solar wind parameters, for example, the dynamic pressure, velocity, density and temperature. In addition, for two spacecraft observations, the locations of BS may affect the resulting asymmetry level. For example, under the same solar wind motional electric field, different intersection angles between projections of two BS locations in MSE Y-Z plane would affect. For Events 1–3, the locations of Tianwen-1 and MAVEN crossings satisfied that one was in the northern hemisphere and the other was near the equator, which makes our analysis easier. More events observed by Tianwen-1 and MAVEN in future will enable further quantitative analysis of the factors determining the asymmetry of the Martian BS.

The explanation of the asymmetric BS may be affected by its movement during the elapsed time between the BS crossings of the two spacecraft. Using magnetic field and plasma parameters from MAVEN, we could estimate the velocity of the BS crossed by MAVEN. We calculated the median value within a 1-min window upstream or downstream of the BS and estimated the BS velocity using the shock mass flux conservation equation (Schwartz, 1998).

$$V_{\mathrm{sh}} = \frac{\Delta(\rho \boldsymbol{V})}{\Delta \rho} \cdot \hat{\boldsymbol{n}}, \tag{7}$$

where ρ is the plasma density, $\boldsymbol{V}$ is the plasma velocity, the Δ notation indicates the jump in any quantity, and $\hat{\boldsymbol{n}}$ is the shock normal, which can be estimated by the coplanarity theorem (Schwartz, 1998):

$$\hat{\boldsymbol{n}} = \pm \frac{(\Delta \boldsymbol{B} \times \Delta \boldsymbol{V}) \times \Delta \boldsymbol{B}}{|(\Delta \boldsymbol{B} \times \Delta \boldsymbol{V}) \times \Delta \boldsymbol{B}|}. \tag{8}$$

This allowed us to estimate the location of the BS near MAVEN at the time of Tianwen-1 crossing. For example, in Event 4, the BS crossed by MAVEN moved outward, so at the time of Tianwen-1 crossing, which occurred after MAVEN crossing, its location might be closer in, indicating a more asymmetric geometry of the BS (see Figure 5a). We found that considering BS motion, the BS in Events 4 and 5 may be more asymmetric, but the BS asymmetry in Events 2 and 3 may be ambiguous (see Table 2). However, it should be noted that the assumed location of the BS near MAVEN at the time of Tianwen-1 crossing depends on the reliability of the estimated shock velocity, which does not account for changes in the shock velocity during the elapsed time. In Event 1, the BS recorded by MAVEN was not simply moving inward or outward, it was oscillating rapidly, making it hard to estimate the shock velocity at each crossing. For this case, we regard the difference of shock locations as its uncertainty, which has little effects on the explanation of asymmetric BS. In addition, we further consider the uncertainty or motion of the BS in the estimation of ΔR_{ss} in Figure 8b.

The explanation of asymmetric BS may be also influenced by other factors. For instance, if the shock surface is wavy, the local location of the BS is farther out or closer in compared to the global geometry. Additionally, the angle between the IMF and the shock normal, θ_{Bn}, may affect the local BS location. A quasi-parallel shock with $\theta_{\mathrm{Bn}} < 45^{\circ}$ may be farther out and may complicate exact identification due to the upstream waves. However, the spatial scale of shock ripples and the effects of θ_{Bn} at Mars require further investigation.

We also checked the asymmetry of the magnetic pileup boundary (MPB) in each event. In Event 1, the locations of the MPB crossed by Tianwen-1 and MAVEN were similar to those of the BS, where MAVEN crossing was near the X-Y plane and Tianwen-1 crossing was in the northern hemisphere and indicated a more inflated shock (Figure 1). For Events 2–5, the locations of the MPB crossed by Tianwen-1 and MAVEN showed no distinct asymmetry. However, it is important to note that (a) the time difference between MPB crossings is tens of minutes, much larger than that of the BS crossings, and (b) the two locations may be close in the Y-Z plane of MSO or MSE reference frames, which may affect the interpretation of potential MPB asymmetry.

6. Conclusions

In this study, we present the direct evidence for an asymmetric Martian bow shock (BS) observed by Tianwen-1 and MAVEN. During the first 2 months of Tianwen-1 observations, we first identified instances where (a) the BS was

Table 2
Effects of Shock Movements on the Explanation of the Shock Asymmetry in Each Event

Event no.	Δt (sec)[a]	Velocity (km s^{-1})[b]	Location	Evaluation
Event 1	−35	unsure[c]	slight inner or outer	asymmetric
Event 2	76	−96	inner	ambiguous
Event 3	−22	28	inner	ambiguous
Event 4	−136	68	inner	more asymmetric
Event 5	−132	277	inner	more asymmetric

Note. The second column shows the elapsed time between MAVEN crossing and Tianwen-1 crossing, where positive/negative values indicate that MAVEN crossed the BS ahead of/behind Tianwen-1. The second column shows the velocity of the BS crossed by MAVEN, where positive/negative values indicate Sun-ward/Mars-ward motion of the BS. The third column shows the relative location of the BS recorded by MAVEN at the time of Tianwen-1 crossing, based on the shock velocity and elapsed time. In the fourth column, we evaluate the BS asymmetry, according to the assumed shock location near MAVEN at the time of Tianwen-1 crossing. [a]$\Delta t = t_{TW1} - t_{MVN}$. [b]positive for Sun-ward, negative for Mars-ward. [c]For Event 1, the bow shock recorded by MAVEN was not simply moving inward or outward, it was oscillating rapidly, it is hard to estimate the shock velocity at each crossing. For this case, we regard the difference of shock locations as its uncertainty.

monitored by the two spacecraft at nearly the same time ($\Delta t < 3$ min) and (b) the crossings could be distinguished using scaled BS shape models. We found three asymmetric BS events that may be caused by the solar wind motional electric field and two asymmetric BS events that may be explained by the hemispherical asymmetry in the Martian crustal magnetic field. We summarized (a) the asymmetry of the BS in the MSE reference frame, where the BS in the northern hemisphere (along the orientation of the solar wind motional electric field) may be more inflated, and (b) the north-south asymmetry of the BS in the MSO reference frame (when the strong crustal field region is at the dayside), where the BS in the southern hemisphere may be more inflated. We quantitatively investigated the relationship between the BS asymmetry and the strength of the solar wind motional electric field. We found that, at least for these three cases, BS asymmetry may increase with the solar wind motional electric field. Further investigations on the asymmetry of the Martian BS should be conducted using more events observed by Tianwen-1 and MAVEN and future multi-spacecraft missions, such as NASA's ESCAPADE mission (Lillis et al., 2019) and ESA's M-MATISSE mission concept (Sanchez-Cano et al., 2022).

Data Availability Statement

The MAVEN data is available at the Planetary Data System (https://pds-ppi.igpp.ucla.edu/mission/MAVEN). The Tianwen-1 data is available at the Lunar and Planetary Data Release System (https://moon.bao.ac.cn/web/enmanager/kxsj?missionName=HX1). The MOMAG data used in this work could also be retrieved from the website of the MOMAG team (https://space.ustc.edu.cn/dreams/tw1_momag).

Acknowledgments
We thank all the individuals who contribute to the science data used in this work. The authors from USTC are supported by the grants from NSFC (42130204, 42188101 and 42404164), the Strategic Priority Program of CAS (XDB41000000) and the Postdoctoral Fellowship Program of CPSF (GZC20241624). LC thanks the support of the Excellent Doctoral Overseas Study Program of USTC. YW is particularly grateful for the support of the New Cornerstone Science Foundation through the Xplorer prize. RL's effort was supported by the Emirates Mars Mission.

References

Cheng, L., Lillis, R., Wang, Y., Mittelholz, A., Xu, S., Mitchell, D. L., et al. (2023). Martian bow shock oscillations driven by solar wind variations: Simultaneous observations from Tianwen-1 and MAVEN. *Geophysical Research Letters*, *50*(16), e2023GL104769. https://doi.org/10.1029/2023GL104769

Connerney, J. E. P., Espley, J., Lawton, P., Murphy, S., Odom, J., Oliversen, R., & Sheppard, D. (2015). The MAVEN magnetic field investigation. *Space Science Reviews*, *195*(1–4), 257–291. https://doi.org/10.1007/s11214-015-0169-4

Dong, Y., Fang, X., Brain, D. A., McFadden, J. P., Halekas, J. S., Connerney, J. E., et al. (2015). Strong plume fluxes at Mars observed by MAVEN: An important planetary ion escape channel. *Geophysical Research Letters*, *42*(21), 8942–8950. https://doi.org/10.1002/2015GL065346

Edberg, N. J. T., Brain, D. A., Lester, M., Cowley, S. W. H., Modolo, R., Fränz, M., & Barabash, S. (2009a). Plasma boundary variability at Mars as observed by Mars global surveyor and Mars express. *Annales Geophysicae*, *27*(9), 3537–3550. https://doi.org/10.5194/angeo-27-3537-2009

Edberg, N. J. T., Eriksson, A. I., Auster, U., Barabash, S., Bößwetter, A., Carr, C. M., et al. (2009b). Simultaneous measurements of Martian plasma boundaries by Rosetta and Mars express. *Planetary and Space Science*, *57*(8–9), 1085–1096. https://doi.org/10.1016/j.pss.2008.10.016

Edberg, N. J. T., Lester, M., Cowley, S. W. H., & Eriksson, A. I. (2008). Statistical analysis of the location of the Martian magnetic pileup boundary and bow shock and the influence of crustal magnetic fields. *Journal of Geophysical Research*, *113*(A8), A08206. https://doi.org/10.1029/2008JA013096

Fang, X., Liemohn, M. W., Nagy, A. F., Ma, Y., De Zeeuw, D. L., Kozyra, J. U., & Zurbuchen, T. H. (2008). Pickup oxygen ion velocity space and spatial distribution around Mars. *Journal of Geophysical Research*, *113*(A2), A02210. https://doi.org/10.1029/2007JA012736

Fang, X., Ma, Y., Masunaga, K., Dong, Y., Brain, D., Halekas, J., et al. (2017). The Mars crustal magnetic field control of plasma boundary locations and atmospheric loss: MHD prediction and comparison with MAVEN. *Journal of Geophysical Research: Space Physics*, *122*(4), 4117–4137. https://doi.org/10.1002/2016JA023509

Garnier, P., Jacquey, C., Gendre, X., Genot, V., Mazelle, C., Fang, X., et al. (2022). The drivers of the Martian bow shock location: A statistical analysis of Mars Atmosphere and volatile EvolutioN and Mars express observations. *Journal of Geophysical Research: Space Physics*, *127*(5), e2021JA030147. https://doi.org/10.1029/2021JA030147

Garnier, P., Jacquey, C., Gendre, X., Génot, V., Mazelle, C., Fang, X., et al. (2022b). The influence of crustal magnetic fields on the Martian bow shock location: A statistical analysis of MAVEN and Mars express observations. *Journal of Geophysical Research: Space Physics*, *127*(5), e2021JA030146. https://doi.org/10.1029/2021JA030146

Gruesbeck, J. R., Espley, J. R., Connerney, J. E. P., DiBraccio, G. A., Soobiah, Y. I., Brain, D., et al. (2018). The three-dimensional bow shock of Mars as observed by MAVEN. *Journal of Geophysical Research: Space Physics*, *123*(6), 4542–4555. https://doi.org/10.1029/2018JA025366

Halekas, J. S., Ruhunusiri, S., Harada, Y., Collinson, G., Mitchell, D. L., Mazelle, C., et al. (2017). Structure, dynamics, and seasonal variability of the Mars-solar wind interaction: MAVEN solar wind ion analyzer in-flight performance and science results. *Journal of Geophysical Research: Space Physics*, *122*(1), 547–578. https://doi.org/10.1002/2016JA023167

Halekas, J. S., Taylor, E. R., Dalton, G., Johnson, G., Curtis, D. W., McFadden, J. P., et al. (2015). The solar wind ion analyzer for MAVEN. *Space Science Reviews*, *195*(1–4), 125–151. https://doi.org/10.1007/s11214-013-0029-z

Hall, B. E. S., Lester, M., Sánchez-Cano, B., Nichols, J. D., Andrews, D. J., Edberg, N. J. T., et al. (2016). Annual variations in the Martian bow shock location as observed by the Mars Express mission. *Journal of Geophysical Research: Space Physics*, *121*(11), 11474–11494. https://doi.org/10.1002/2016JA023316

Hall, B. E. S., Sánchez-Cano, B., Wild, J. A., Lester, M., & Holmström, M. (2019). The Martian bow shock over solar cycle 23–24 as observed by the Mars express mission. *Journal of Geophysical Research: Space Physics*, *124*(6), 4761–4772. https://doi.org/10.1029/2018JA026404

Langlais, B., Thébault, E., Houliez, A., Purucker, M. E., & Lillis, R. J. (2019). A new model of the crustal magnetic field of Mars using MGS and MAVEN. *Journal of Geophysical Research: Planets*, *124*(6), 1542–1569. https://doi.org/10.1029/2018JE005854

Lillis, R. J., Curry, S., Curtis, D. W., Taylor, E., Parker, J., Luhmann, J. G., et al. (2019). ESCAPADE: Coordinated multipoint observations of the Martian magnetosphere. *AGU fall meeting*, SM42B.

Liu, K., Hao, X. J., Li, Y. R., Zhang, T. L., Pan, Z. H., Chen, M. M., et al. (2020). Mars orbiter magnetometer of China's first Mars mission Tianwen-1. *Earth and Planetary Physics*, *4*(4), 384–389. https://doi.org/10.26464/epp2020058

Mazelle, C., Winterhalter, D., Sauer, K., Trotignon, J. G., Acuña, M. H., Baumgärtel, K., et al. (2004). Bow shock and upstream phenomena at Mars. *Space Science Reviews*, *111*(1/2), 115–181. https://doi.org/10.1023/B:SPAC.0000032717.98679.d0

Mitchell, D. L., Mazelle, C., Sauvaud, J. A., Thocaven, J. J., Rouzaud, J., Fedorov, A., et al. (2016). The MAVEN solar wind electron analyzer. *Space Science Reviews*, *200*(1–4), 495–528. https://doi.org/10.1007/s11214-015-0232-1

Ramstad, R., Barabash, S., Futaana, Y., & Holmström, M. (2017). Solar wind- and EUV-dependent models for the shapes of the Martian plasma boundaries based on Mars Express measurements. *Journal of Geophysical Research: Space Physics*, *122*(7), 7279–7290. https://doi.org/10.1002/2017JA024098

Sanchez-Cano, B., Opgenoorth, H., Leblanc, F., Andrews, D., & Lester, M. (2022). The M-MATISSE mission: Mars magnetosphere ATmosphere ionosphere and surface SciencE. In *44th COSPAR scientific assembly* (pp. B4.3-0019–0022).

Schwartz, S. J. (1998). Shock and discontinuity normals, Mach numbers, and related parameters. *ISSI Scientific Reports Serie*, *1*, 249–270.

Simon Wedlund, C., Volwerk, M., Beth, A., Mazelle, C., Möstl, C., Halekas, J., et al. (2022). A fast bow shock location predictor-estimator from 2D and 3D analytical models: Application to Mars and the MAVEN mission. *Journal of Geophysical Research: Space Physics*, *127*(1), e2021JA029942. https://doi.org/10.1029/2021JA029942

Sui, H. Y., Wang, M., Lu, J. Y., Zhou, Y., & Wang, J. (2023). Interplanetary magnetic field effect on the location of the Martian bow shock MAVEN observations. *The Astrophysical Journal*, *945*(2), 136. https://doi.org/10.3847/1538-4357/acbd4c

Trotignon, J. G., Mazelle, C., Bertucci, C., & Acuña, M. H. (2006). Martian shock and magnetic pile-up boundary positions and shapes determined from the Phobos 2 and Mars Global Surveyor data sets. *Planetary and Space Science*, *54*(4), 357–369. https://doi.org/10.1016/j.pss.2006.01.003

Vignes, D., Acuna, M. H., Crider, D. H., Connerney, J., Reme, H., & Mazelle, C. (2002). Factors controlling the location of the bow shock at Mars. *Geophysical Research Letters*, *29*(9), 1–4. https://doi.org/10.1029/2001gl014513

Vignes, D., Mazelle, C., Rme, H., Acuña, M. H., Connerney, J. E. P., Lin, R. P., et al. (2000). The solar wind interaction with Mars: Locations and shapes of the bow shock and the magnetic pile-up boundary from the observations of the MAG/ER experiment onboard Mars global surveyor. *Geophysical Research Letters*, *27*(1), 49–52. https://doi.org/10.1029/1999GL010703

Wang, G., Xiao, S., Wu, M., Zhao, Y., Jiang, S., Pan, Z., et al. (2024). Calibration of the zero offset of the fluxgate magnetometer on board the Tianwen-1 orbiter in the Martian magnetosheath. *Journal of Geophysical Research: Space Physics*, *129*(1), e2023JA031757. https://doi.org/10.1029/2023JA031757

Wang, M., Xie, L., Lee, L. C., Xu, X. J., Kabin, K., Lu, J. Y., et al. (2020). A 3D parametric Martian bow shock model with the effects of Mach number, dynamic pressure, and the interplanetary magnetic field. *The Astrophysical Journal*, *903*(2), 125. https://doi.org/10.3847/1538-4357/abbc04

Wang, Y., Zhang, T., Wang, G., Xiao, S., Zou, Z., Cheng, L., et al. (2023). The Mars orbiter magnetometer of Tianwen-1: In-flight performance and first science results. *Earth and Planetary Physics*, *7*(2), 1–13. https://doi.org/10.26464/epp2023028

Zou, Z., Wang, Y., Zhang, T., Wang, G., Xiao, S., Pan, Z., et al. (2023). In-flight calibration of the magnetometer on the Mars orbiter of Tianwen-1. *Science China Technological Sciences*, *66*(8), 2396–2405. https://doi.org/10.1007/s11431-023-2401-2